A typical result is given in Fig. 2. The above assumption about the receiver noise parameter dependence with frequency can be simply checked on this result. At each maximum F_M, or minimum F_m, we observe the same magnitude on the whole bandwidth. Adding the cold load measurement, we obtain three conditions from the whole classical expression

$$F = F_{min} + \frac{4R_n}{Z_0} \frac{|\Gamma_S - \Gamma_{opt}|^2}{|1+\Gamma_{opt}|^2(1-|\Gamma_S|^2)}$$

where F_{min} is the minimum noise figure, R_n is the noise equivalent resistance, Z_0 is the reference impedance and Γ_{opt} is the optimum source reflection coefficient. F is minimum (F_m) when Γ_s and Γ_{opt} have the same phase (point (i)), F is maximum (F_M) when Γ_s and Γ_{opt} have opposite phases (point (ii)) and $F = F_{50}$ when 50Ω is connected. One obtains $\Phi(\Gamma_{opt})$ from the known phase of Γ_{sc} at point (i), leading to three equations for three scalar unknowns $|\Gamma_{opt}|$, R_n and F_{min}.

Table 1: Dispersion of four noise parameters of receiver

Frequency	kBG_0(E-12)	F_{min}	Rn	$\|\Gamma_{opt}\|$	$\Phi(\Gamma_{opt})$
GHz	W/K	dB	Ω		rad
6	5.5±0.84	2.94±0.13	6.98±0.43	0.82±0.07	-23.14±0.07
8	1.28±0.02	4.03±0.10	34.80±7.27	0.22±0.03	-31.52±0.06
10	1.87±0.10	4.41±0.10	16.48±2.62	0.18±0.01	-39.62±0.04
12	1.85±0.05	4.56±0.27	18.67±6.07	0.25±0.03	-48.69±0.05
14	3.93±0.08	3.79±0.10	68.82±15.80	0.28±0.08	-56.18±0.11

Receiver noise measurements: Results for four noise parameters of receiver and kBG_0 associated are collected in Table 1. The observed dispersions are nearly 0.2dB, 20% and 0.1 rad on F_{min}, $|\Gamma_{opt}|$ and $\Phi(\Gamma_{opt})$, respectively. These measurements have been carried out under various conditions (different offset shorts at different time).

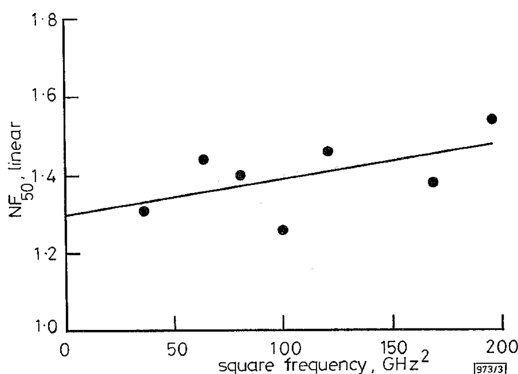

Fig. 3 *50Ω noise figure against square of frequency (FHX13X transistor)*

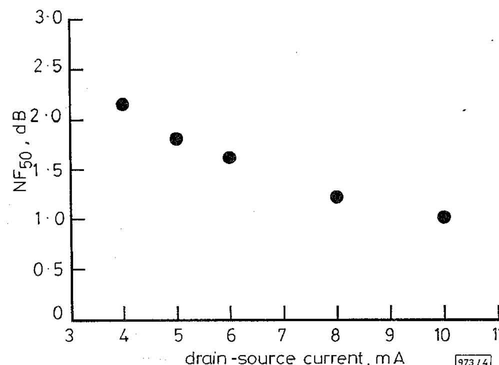

Fig. 4 *50Ω noise figure against drain-source current (FHX13X transistor)*

V_{ds} = 2V
Frequency = 10GHz

50Ω noise figure results on HEMTs: Preliminary results on Fujitsu (FHX13X) pseudomorphic HEMTs on a GaAs substrate are presented in Figs. 3 and 4. In Fig. 3 the extrapolated value at the origin gives an estimation [1] of R_n = 12Ω ± 2Ω which is in good agreement with the manufacturer values. The variation of the F_{50} calculated with drain current I_{ds} is shown in Fig. 4. The measurement dispersions are estimated to be ±0.2dB. The smooth behaviour and the agreement with manufacturer values confirms the receiver calibration accuracy. Similar results have been obtained on a NE32400 transistor.

Conclusion: A new 50Ω noise measurement method has been proposed. This method does not use a tuner nor a circulator, thus enabling a broad-band study. This approach is particularly suitable for accurate low temperature noise measurements which will be presented in the future.

© IEE 1996
27 September 1995
Electronics Letters Online No: 19960146

P. Crozat, V. Danelon, A. Sylvestre and G. Vernet (*Institut d'Electronique Fondamentale, URA 22 du CNRS, Université Paris Sud, 91405 Orsay, France*)

C. Boutez (*DEMIRM, Observatoire de Paris, 61 Avenue de l'Observatoire, 75014 Paris, France*)

M. Chaubet (*CNES, 18 Avenue E. Belin, 31055 Toulouse Cedex, France*)

References

1 DAMBRINE, G., HAPPY, H., DANNEVILLE, F., and CAPPY, A.: 'A new method for on wafer noise measurement', *IEEE Trans.*, 1993, **MTT-41**, (3), pp. 375–381

2 TASKER, P.J., REINERT, W., HUGHES, B., BRAUNSTEIN, J., and SCHLECHTWEG, M.: 'Transistor noise parameter extraction using a 50Ω measurement system'. IEEE MTT-S Int. Microw. Symp. Digest, 1993, pp. 1251–1254

3 CROZAT, P., BOUCHON, D., HENAUX, J.C., ADDE, R., and VERNET, G.: 'Cryogenic on-wafer microwave network analyzer high precision measurements (0.1–40GHz) of microelectronic devices'. Proc. Low Temp. Electron. and High Temp. Superconductivity, (Ed. Electrochem. Soc.), 1993, **93-22**, pp. 283–293

4 MEIERER, R., and TSIRONIS, C.: 'An on-wafer noise parameter measurement technique with automatic receiver calibration', *Microw. J.*, 1995, pp. 22–37

Measurement of refractive index of GaSb (1.8 to 2.56μm) using a prism

M. Muñoz Uribe, C.E.M. de Oliveira, J.H. Clerice, R.S. Miranda, M.B. Zakia, M.M.G. de Carvalho and N.B. Patel

Indexing terms: Refractive index, Refractive index measurement, Semiconductor devices

The authors have measured the refractive index of GaSb for the transparent region from 1.8 to 2.56μm using refraction in a prism. The values obtained agree well with those recently measured by the authors using ellipsometry. A good fit to the experimental data is obtained using the single oscillator model.

Introduction: GaSb and its lattice matched quaternaries GaAlAsSb and GaInAsSb are employed [1] in various optoelectronic devices such as lasers and detectors which incorporate optical waveguides. The design and analysis of such devices requires [2] accurate knowledge of the refractive indices and their variation with wavelength for the different layers which compose the waveguide. There are very few reports [3 – 5] in the literature reporting measurements of the refractive index of GaSb in the transparent region. For unknown reasons there is a large dispersion in the values reported in these previous works. An accurate determination of the refractive index of GaSb is lacking, and is needed for the correct determination of the refractive index of thin films grown on GaSb substrates. In this Letter we report measurements of the refractive index of p-type GaSb ($1.0 \times 10^{17}cm^{-3}$ at 300K) in the 1.8 to 2.56μm wavelength range, using refraction of light in a prism.

Experimental details: The prism was cut from 25 mm diameter single crystal grown in our laboratory [6] The crystal was nominally undoped with a residual p-type carrier concentration of $1.0 \times 10^{17} cm^{-3}$. The two faces of the prism were polished to a mirror finish. The determination of the prism angle A (Fig. 1) was made with the prism mounted on the centre stage of a Rudolph Ellipsometer model 436. Light from an He-Ne laser was reflected from a prism face to double back over itself. The centre stage was then rotated through an angle necessary for repeating the reflection adjustment from the other prism face. The difference between 180° and this angle gives the prism angle A, which was determined to be 6.53° ± 0.01°.

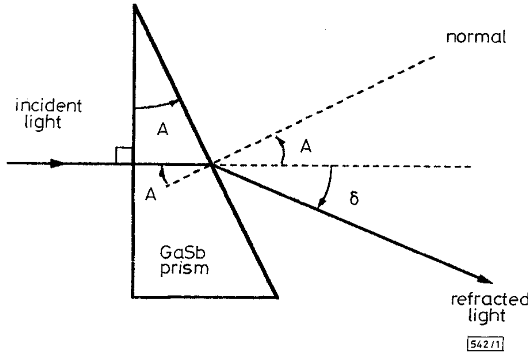

Fig. 1 *Geometry of experiment*

The geometry used for the determination of the refractive index is shown in Fig. 1. The prism was mounted again on the centre stage and the angle δ of the refracted light was determined by an LN_2 cooled InAs detector mounted on the rotating arm of the ellipsometer base. Light at different wavelengths was obtained from a McPherson monochromator model 218. A bandwidth of 90Å was used in all measurements. A light chopper and a lock-in amplifier were used to improve the sensitivity of the detection. With this arrangement the angle δ was determined with an accuracy better than 0.01°. Applying the Snell law to the geometry of Fig. 1, the refractive index of the prism is given by

$$n = \frac{\sin(A+\delta)}{\sin A}$$

The resolution in n determined by the experimental setup was estimated to be ±0.005.

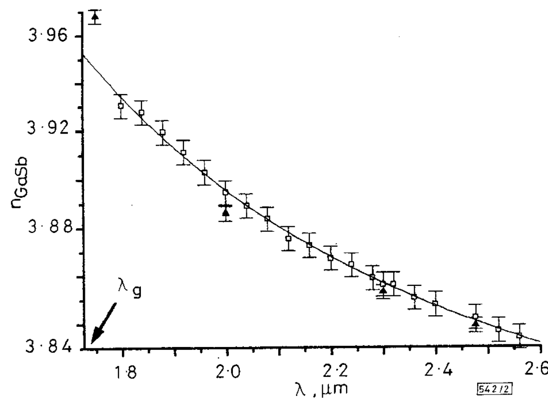

Fig. 2 *Fit of prism data by single oscillator model and comparison with ellipsometric measurements*

▲ ellipsometric technique
□ prism technique
——— single oscillator model for prism data
λ_g is wavelength corresponding to GaSb gap

Results and analysis: The refractive index data obtained against the wavelength are shown in Fig. 2. Also shown are the four values at wavelengths of 1.75, 2.0, 2.3 and 2.477μm reported recently by us [7] using ellipsometry on a p-type sample with $1.5 \times 10^{15} cm^{-3}$ carrier concentration at 300K. The present measurements of transmission through the prism showed that light at 1.75μm suffers considerable absorption, reducing the signal to below our measurement capacity. This throws some doubt on the value obtained by ellipsometry for this wavelength, since the analysis there was carried out under the assumptions of no absorption in the sample. The others points are in good agreement with the present prism measurements.

The continuous line in Fig. 2 is a parametrical fit to the data points using the so-called single oscillator model [8], which assumes that in the limit of small frequency the dielectric constant ($\varepsilon = n^2$) can be described by $\varepsilon(E) = 1 + (E_0 E_d)/(E_0^2 - E^2)$, where E_0 and E_d are two empirical parameters and E is the photon energy. In this case E_0 = 2.17eV and E_d = 28.27eV. The fit is quite good, even at higher frequencies near the band-edge.

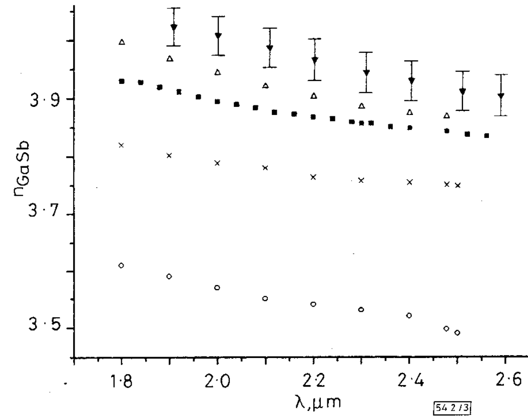

Fig. 3 *Comparison of measurements of GaSb refractive index by different authors*

Error bar accounts for error in retrieving data from original very condensed graphic
▼ Oswald data
△ Alibert data
■ our prism data
× Edwards prism data
○ Edwards reflectance data

Discussion: In Fig. 3 we compare our prism data with the results of Edwards *et al.* [3] ($p \simeq 10^{17} cm^{-3}$), Oswald *et al.* [4] ($p \simeq 10^{17} cm^{-3}$) and Alibert *et al.* [5] ($p \simeq 10^{17} cm^{-3}$). In all these cases a reflectivity type technique was used, while Edwards also made measurements based on the minimum deviation angle of a GaSb prism. A great lack of concordance in these data is observed. Our prism measurements are direct and simple, and not subject to errors caused by the presence of surface oxide layers or light source intensity variations.

As we stated before, an inaccurate value for the refractive index of GaSb would mislead the determination of the index for any thin film grown on GaSb substrates. This is a timely matter because currently there are efforts to develop GaInAsSb/GaAlAsSb/GaSb double heterojunction lasers, emitting in the region above 2.0μm. The index step required to waveguide the radiation is a very important input for designing and evaluating the performance of such lasers [2]. For this purpose, a precise determination of the refractive indices of the compounds involved in the laser structure is necessary.

Conclusion: In this Letter we have presented the measurements of the refractive index of GaSb made by a prism technique. The results agree well with our previous measurements using ellipsometry. A good fitting to the data was obtained using the single oscillator model.

Acknowledgments: We would like to acknowledge the technical discussions and suggestions of N. Frateschi and the financial support of CNPq, FINEP, CPqD/TELEBRAS and CONACyT (Mexican Agency).

© IEE 1996
21 November 1995
Electronics Letters Online No: 19960176

M. Muñoz Uribe, C.E.M. de Oliveira, J.H. Clerice, R.S. Miranda, M.B. Zakia, M.M.G. de Carvalho and N.B. Patel (*Instituto de Física 'Gleb Wataghin', Univeridade Estadual de Campinas, Unicamp Campinas 13081-970, SP, Brazil*)

M. Muñoz Uribe: Permanent address: Departamento de Matemáticas, Universidad Autonoma Metropolitana-Azcapotzalco, Av. San Pablo 180, DF, Mexico

References

1 MILNES, A.G., and POLIAKOV, A.Y.: 'Review: Gallium antimonide device related properties', *Solid State Electron.*, 1993, **36**, pp. 803–818

2 LOURAL, S.S., MOROZINI, M.B.Z., HERRERA-PÉREZ, J.L., VON ZUBEN, A.A.G., DA SILVEIRA, A.C., and PATEL, N.B.: 'Refractive index step and optical confinement in $Ga_{0.86}In_{0.14}As_{0.13}Sb_{0.87}$/$Ga_{0.73}Al_{0.27}As_{0.02}Sb_{0.98}$ double heterostructure lasers emitting at 2.2μm', *Electron. Lett.*, 1993, **29**, (14), pp. 1240–1241

3 EDWARDS, D.F., and HAYNE, G.S.: 'Optical properties of gallium antimonide', *J. Opt. Soc. Am.*, 1959, **49**, pp. 414–415

4 OSWALD, , and SCHADE, R.: 'Über die bestimmung der optischen konstanten von halbleitern des typus $A^{III}B^{V}$ im infraroten', *Z. Naturforsh*, 1954, **9a**, pp. 611–617

5 ALIBERT, , SKOURI, M., JOULLIE, A., BENOUNA, M., and SADIQ, S.: 'Refractive indices of AlSb and GaSb-lattice matched $Al_xGa_{1-x}As_ySb_{1-y}$ in the transparent wavelength region', *J. Appl. Phys.*, 1991, **69**, (5), pp. 3208–3211

6 DE OLIVEIRA, E.M., and DE CARVALHO, M.M.G.: 'A simple technique for Czochralski growth of GaSb single crystals from scum-free melt', *J. Cryst. Growth*, 1995, **151**, pp. 9–12

7 MUÑOZ URIBE, M., MIRANDA, R.S., ZAKIA, M.B., DE SOUZA, C.F., RIBEIRO, C.A., CLERICE, J.H., and PATEL, N.B.: 'Near band gap refractive index of GaSb', *Materials Sci. Eng B*, (accepted for publication)

8 WEMPLE, H., and DIDOMENICO, Jr., M.: 'Behavior of the electronic dielectric constant in covalent and ionic materials', *Phys. Rev. B*, 1971, **3**, (4), pp. 1338–1351

MOS device conductance modelling technique for an accurate and efficient mixed-mode simulation of CMOS circuits

G. Samudra and Teng Kiat Lee

Indexing terms: Semiconductor device models, CMOS integrated circuits

A new technique for modelling the conductance of an MOS device for the electrical logic simulation (the Elogic algorithm) of CMOS circuits is proposed. The technique is general and applicable to any analytic device current model. The Elogic algorithm allows the representation of a logic transition using a finite number of voltage steps and calculates time for each transition between the adjacent voltage steps. The examples show that the new technique can correctly predict a complete electrical waveform with a large voltage step of 1V to yield at least an order of magnitude computational time advantage over the circuit simulation.

Introduction: Nowadays, with VLSI, it is no longer possible for a circuit designer to work without computer-aided design (CAD) tools. The first and foremost emphasis of CAD tool development must be design verification. Simulators belong to the category of design verification tool and they can be further subdivided into different simulation levels: (i) electrical, (ii) switch, (iii) logic, and (iv) behavioural, this order is in terms of the decreasing amount of information, accuracy and computational overhead. The logic simulation normally considers only two states and is adequate for the functional verification with very little timing information. The Elogic algorithm [1 – 5] is an enhanced switch level simulation technique which bridges the gap between the electrical level simulation and logic simulation with computational time comparable to that of logic simulation. The Elogic algorithm represents a MOS device using conductance. This Letter presents a technique for modelling the conductances in an Elogic algorithm so as to achieve accuracy comparable to electrical level simulation, with a computational time advantage of at least an order of magnitude.

Elogic simulation method: In addition to this speed advantage, the Elogic simulation algorithm is applicable to circuits such as precharge networks, pass-transistor networks, and bi-directional circuits, all of which cannot be handled by a logic simulator. Owing to the use of an event-driven selective trace scheduling scheme and its higher level of abstraction than the traditional electrical simulators such as SPICE, switch level simulators can achieve much higher speed.

Unlike conventional electrical level simulators, where the voltage change at a node is calculated at the end of a time-step, Elogic solves for the amount of time needed to make a transition from one voltage state to another. The important factor that determines the accuracy of Elogic is the number of discrete levels chosen in the voltage space. For example, in digital applications with voltages between 0 and 5V, having a 0.1V voltage step between levels will achieve greater accuracy than having a 1V voltage step at the expense of the computer time. Voltages between the discrete levels are approximated by piece-wise linear segments. Circuit nodes are only allowed to make a transition from one state to an adjacent state.

Improvement in simulation accuracy can also be achieved by using good models for devices. In Elogic, models exist for transistors, nodes, and capacitances. During transient simulation, Elogic linearises all non-linear circuit elements such as the transistors by converting them into their small-signal models with a current source and the device conductance in parallel, or a Thevenin equivalent voltage source and the same conductance in series. The capacitance at every node is also replaced by a constant voltage source. The Thevenin equivalent voltage determines if a transition to an adjacent voltage is necessary. When a transition is needed, the time for the node to make the transition is calculated from the equation governing the current flow through the capacitance at that node.

Device conductance modelling: In the existing technique a constant voltage source is used to represent the fan-in nodes such as the gate of the transistor (V_G). The conductance $g_{m,vds}$ is calculated by taking the value of $\partial I_{DS}/\partial V_{DS}$ at the voltage conditions at the beginning of the event. The consequence of this conductance modelling technique, when the voltage step-size is large and the gate voltage is rising, is that we will consistently under-estimate the conductances of n-channel transistors and over-estimate the conductances of p-channel transistors. For a falling gate voltage, the opposite effect is observed. The result of these two effects is the unbounded increase in error for delay calculations. Hence a voltage step of 0.1V or lower becomes essential to predict a reasonably accurate electrical waveform.

The main contribution of this Letter is to provide a more realistic estimation of $g_{m,vds}$ to achieve sufficient accuracy with a voltage step of 1 V, when the movements of fan-in nodes such as V_G are known *a-priori*. Instead of using the conductance value at the present state of the fan-in node, a more realistic average value of the conductance over the voltage step is used. i.e.

$$\bar{g}_{m,vds} = \frac{\int_{V_{GS1}}^{V_{GS2}} \frac{\partial I_{DS}}{\partial V_{DS}} dV_{GS}}{V_{GS2} - V_{GS1}}$$

Clearly, the calculation is general and will work in the case of any well behaved analytic drain current model.

Table 1: Run times for different simulation techniques for various circuits

Ring oscillator	ITA	Traditional Elogic (1V step)	Traditional Elogic (0.1V step)	New technique (1V step)
s	1.48	0.1	0.81	0.13

Long chain of 30 inverters	ITA	Traditional Elogic (1V step)	Traditional Elogic (0.1V step)	New technique (1V step)
s	3.76	0.79	0.33	0.24

Arbitrary chain of four logic gates	ITA	Traditional Elogic (1V step)	New technique (1V step)
s	0.32	0.08	0.06